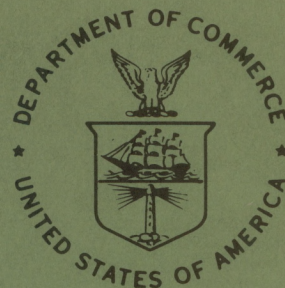


A
QC
879.5
U4
no.96

OAA Technical Memorandum NESS 96



SATELLITE DATA SET FOR SOLAR
INCOMING RADIATION STUDIES

Washington, D.C.
May 1978

noaa

NATIONAL OCEANIC AND
ATMOSPHERIC ADMINISTRATION

/ National Environmental
Satellite Service

NOAA TECHNICAL MEMORANDUMS

National Environmental Satellite Service Series

The National Environmental Satellite Service (NESS) is responsible for the establishment and operation of the environmental satellite systems of NOAA.

NOAA Technical Memorandums facilitate rapid distribution of material that may be preliminary in nature and so may be published formally elsewhere at a later date. Publications 1 through 20 and 22 through 25 are in the earlier ESSA National Environmental Satellite Center Technical Memorandum (NESCTM) series. The current NOAA Technical Memorandum NESS series includes 21, 26, and subsequent issuances.

Publications listed below are available from the National Technical Information Service, U.S. Department of Commerce, Sills Bldg., 5285 Port Royal Road, Springfield, Va. 22161. Prices on request. Order by accession number (given in parentheses). Information on memorandums not listed below can be obtained from Environmental Data Service (D822), 6009 Executive Boulevard, Rockville, MD 20852.

- NESS 61 Potential Value of Earth Satellite Measurements to Oceanographic Research in the Southern Ocean. E. Paul McClain, January 1975, 18 pp. (COM-75-10479/AS)
- NESS 62 A Comparison of Infrared Imagery and Video Pictures in the Estimation of Daily Rainfall From Satellite Data. Walton A. Follansbee and Vincent J. Oliver, January 1975, 14 pp. (COM-75-10435/AS)
- NESS 63 Snow Depth and Snow Extent Using VHRR Data From the NOAA-2 Satellite. David F. McGinnis, Jr., John A. Pritchard, and Donald R. Wiesnet, February 1975, 10 pp. (COM-75-10482/AS)
- NESS 64 Central Processing and Analysis of Geostationary Satellite Data. Charles F. Bristor (Editor), March 1975, 155 pp. (COM-75-10853/AS)
- NESS 65 Geographical Relations Between a Satellite and a Point Viewed Perpendicular to the Satellite Velocity Vector (Side Scan). Irwin Ruff and Arnold Gruber, March 1975, 14 pp. (COM-75-10678/AS)
- NESS 66 A Summary of the Radiometric Technology Model of the Ocean Surface in the Microwave Region. John C. Alishouse, March 1975, 24 pp. (COM-75-10849/AS)
- NESS 67 Data Collection System Geostationary Operational Environmental Satellite: Preliminary Report. Merle L. Nelson, March 1975, 48 pp. (COM-75-10679/AS)
- NESS 68 Atlantic Tropical Cyclone Classifications for 1974. Donald C. Gaby, Donald R. Cochran, James B. Lushine, Samuel C. Pearce, Arthur C. Pike, and Kenneth O. Poteat, April 1975, 6 pp. (COM-75-1676/AS)
- NESS 69 Publications and Final Reports on Contracts and Grants, NESS-1974. April 1975, 7 pp. (COM-75-10850/AS)
- NESS 70 Dependence of VTPR Transmittance Profiles and Observed Radiances on Spectral Line Shape Parameters. Charles Braun, July 1975, 17 pp. (COM-75-11234/AS)
- NESS 71 Nimbus-5 Sounder Data Processing System, Part II: Results. W. L. Smith, H. M. Woolf, C. M. Hayden, and W. C. Shen. July 1975, 102 pp. (COM-75-11334/AS)
- NESS 72 Radiation Budget Data From the Meteorological Satellites, ITOS 1 and NOAA 1. Donald H. Flanders and William L. Smith, August 1975, 22 pp. (PB-246877/AS)
- NESS 73 Operational Processing of Solar Proton Monitor Data. Stanley R. Brown, September 1975. (Revision of NOAA TM NESS 49), 15 pp. (COM-73-11941)
- NESS 74 Monthly Winter Snowline Variation in the Northern Hemisphere from Satellite Records, 1966-75. Donald R. Wiesnet and Michael Matson, November 1975, 21 pp. (PB-248437)
- NESS 75 Atlantic Tropical and Subtropical Cyclone Classifications for 1975. D. C. Gaby, J. B. Lushine, B. M. Mayfield, S. C. Pearce, and K. O. Poteat, March, 1976, 14 pp. (PB-253968/AS)

(Continued on inside back cover)

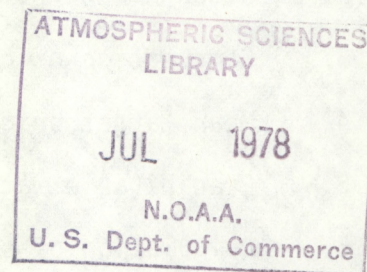
A
QC
879.5
U4
no. 96

NOAA Technical Memorandum NESS 96

SATELLITE DATA SET FOR SOLAR
INCOMING RADIATION STUDIES

J. Dan Tarpley, Stanley R. Schneider,
J. Emmett Bragg, and Marshall P. Waters, III

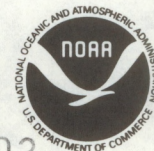
Washington, D.C.
May 1978



UNITED STATES
DEPARTMENT OF COMMERCE
Juanita M. Kreps, Secretary

NATIONAL OCEANIC AND
ATMOSPHERIC ADMINISTRATION
Richard A. Frank, Administrator

National Environmental
Satellite Service
David S. Johnson, Director



78

2403

CONTENTS

List of tables	iv
List of figures.	iv
Abstract	1
1. The joint NESS/GPC solar insolation experiment.	1
2. Description of the satellite and sensor	2
3. The VISSR data base (VDB)	2
4. Description of the study area	3
5. Satellite and conventional meteorological data collection	5
5.1. Determination of target clear radiances	7
5.1.1. Data collection	7
5.1.2. Determination of regression coefficients.	7
5.2. Cloud amount.	8
5.3. Computation of cloud brightness	11
5.4. Mean target brightness.	11
5.5. Precipitable water and surface pressure	11
5.6. Calculation of solar zenith and azimuth angles.	11
6. Results of summer 1977 collection effort.	12
7. Quality control	14
7.1. VISSR data.	14
7.2. Test data	17
8. Data tape format.	17
9. Pyranometer data.	20
10. Summary	21
Acknowledgments.	21
References	21
Appendix A. Regression coefficients for predicting clear radiance . . .	23

Appendix B. Date and time of pictures	25
Appendix C. Examples of each data type.	29

TABLES

1. The experimental VISSR data base (VDB)	3
2. Breakdown of lost days of data	12
3. Breakdown of possible time slots	14

FIGURES

1. Area covered by surface insolation experiment.	4
2. One-km GOES-1/VISSR image taken over the test area on September 30, 1977.	6
3. Procedure for obtaining clear-radiance coefficients for a specific target.	9
4. Illumination angles used in regressing for visible clear radiance .	10
5. Histogram showing the daily number of pictures successfully utilized during the test period.	13
6. Predicted and measured satellite responses for a selected target at 1600Z.	15
7. Predicted and measured satellite responses for a selected target at 2100Z.	16
8. Computer printout of a 1600Z VISSR image on April 25, 1977	18
9. A 4-km resolution VISSR image used for data registration	19

SATELLITE DATA SET FOR SOLAR INCOMING RADIATION STUDIES

J. Dan Tarpley, Stanley R. Schneider,
J. Emmett Bragg, and Marshall P. Waters, III
National Environmental Satellite Service, NOAA
Washington, D.C.

ABSTRACT. The National Environmental Satellite Service (NESS) collected and processed Geostationary Operational Environmental Satellite (GOES) data in the summer of 1977 as part of a joint experiment with the Great Plains Agricultural Council (GPC) to determine if incoming solar radiation could be inferred from satellite data. The satellite data collection effort entailed the calculation of cloud amount, cloud brightness, mean target brightness, precipitable water, and surface pressure for 50-km areas over the Great Plains. Sixty-three days of satellite data were collected. A coincident set of pyranometer data was obtained by the GPC.

1. THE JOINT NESS/GPC SOLAR INSOLATION EXPERIMENT

The NESS has undertaken a joint experiment with the GPC to determine if incoming solar radiation at the surface can be inferred using satellite data. The study is divided into two parts, a data-gathering effort and an analysis effort. This report discusses the recording and processing of the satellite measurements for the data collection part of the experiment.

Insolation (incoming solar radiation) is defined as the rate at which direct and scattered solar radiation is incident upon a unit horizontal surface and is measured in units of energy/area·second. Insolation at the Earth's surface in the visible region of the solar spectrum is one of the most important meteorological variables determining growth rate of crops. The ultimate use for satellite-inferred insolation is measurement of the spatial distribution of radiation for large-scale estimates of potential evapotranspiration and photosynthesis.

Insolation is also the quantity of interest in estimating the solar energy available at specific locations. For example, detailed insolation data are needed for finding optimum sites for solar power plants.

The NESS/GPC experiment entailed the collection of coincident satellite, conventional meteorological, and pyranometer data over the Great Plains during the summer of 1977. The conventional meteorological data and the satellite measurements were those expected to contain the most information relating to surface insolation. Scene brightness, cloud brightness, and cloud amount were computed from satellite data. Surface pressure and precipitable water were obtained from the National Meteorological Center (NMC), and ground truth measurements of insolation were made with the GPC pyranometer network.

2. DESCRIPTION OF THE SATELLITE AND SENSOR

Two geostationary meteorological satellites operated by NESS, the Synchronous Meteorological Satellite/Geostationary Operational Environmental Satellite (SMS-2/GOES-2), view the Earth's disk through Visible and Infrared Spin-Scan Radiometer (VISSR) instruments. A description of this dual geostationary satellite system can be found in Technical Memorandum NESS 64 (Bristor 1975). The satellites, GOES-2 and SMS-2, were fixed over the equator at 75°W and 135°W, respectively, at an altitude of about 37,500 km.

The VISSR instrument provides concurrent observations in the infrared (IR) spectrum (10.5 to 12.6 μm) and in the visible (VIS) spectrum (0.55 to 0.75 μm). The IR data are expressed as eight-bit count values that can be converted to equivalent blackbody temperatures. The VIS data are expressed as six-bit count values measuring relative brightness. Information is also appended to the data that allows the values to be located with respect to the Earth's surface.

3. THE VISSR DATA BASE (VDB)

The digital VISSR data, at reduced resolution from the eastern and western satellites, are being processed into an experimental VDB. Data may be obtained from each satellite at 30-minute intervals. About 18 minutes are required for the VISSR to produce the digital image or "picture" of the full disk. The western satellite's data are normally acquired at 15 minutes and 45 minutes after the hour, while the eastern satellite's data are acquired on the hour and half hour. Data from the full Earth's disk are currently reduced to areas extending from 50°N-50°S latitude and approximately 50° longitude east and west of the satellite subpoints. These stored arrays of digital data will be referred to as "pictures."

The VDB is formed by processing data ingested in real time from the SMS/GOES satellites onto computer disks. Data at full resolution are received at Suitland, Maryland, via two 7-m dish antennas. The data then pass through interfacing electronics to the VISSR ingest computers (sectorizers), where the resolution of the VIS channel is reduced from 1 km to 4 km. The resolution of the IR channel at this stage is still 4x8 km. The data are then passed to NOAA's IBM S360/195 computer via a direct-memory interface unit and software known as the real-time monitor. The software that actually builds the VDB takes data from a staging disk formed by the real-time monitor, reduces both the VIS and IR channels to 8-km resolution, and places the data on computer disks. When data are placed in the VDB in this manner, they can normally be accessed for use about 3 minutes after the end of the picture or about 22 minutes after the start of the picture. Some data in the VDB are placed there via magnetic tape and would be available for use about one hour after picture start time. It should also be noted that the VDB also contains selected, 4-km VIS pictures.

The VDB physically resides on four disk packs that comprise a portion of the NOAA IBM S360/195 computer facility at Suitland. The data are maintained for 24 hours. After 24 hours, a selected portion of the data is archived on

magnetic tape for the Environmental Data Service (EDS); the remaining data are overwritten on disk with current data. The characteristics of the experimental VDB are summarized in table 1.

Table 1.--The experimental VISSR Data Base (VDB)

Satellite	Subpoint	Acquisition times	Data coverage	Data residence time
East (GOES-2)	75°W	On the hour and selected half-hour pictures	50°N-50°W; 25°W-125°W	24 hr
West (SMS-2)	125°W	15 minutes after the hour and selected 45-minutes after-the-hour pictures	50°N-50°S; 85°W-175°E	24 hr

Sensor Data Characteristics:

Data type	Spectral interval	Units	Convertible to	Nominal subpoint spatial resolution
IR	10.5-12.6 μ m	8-bit count values	Equivalent blackbody radiative temperatures	8 km
VIS	0.55-0.75 μ m	6-bit count values	Albedo	8 km

Other Characteristics:

- Earth location and calibration information are appended.
- Resides on four disk packs in the NOAA IBM S360/195 computer system.
- Currently, some 95 of the possible 144 pictures are processed.
- The processing system, format, and data coverages are experimental and, thus, are subject to interruption at any time by operational priorities and requirements.
- 0930Z, 1000Z, 1600Z, 2130Z, 2200Z IR and 1600Z VIS are archived for EDS.
- 1015Z, 1045Z, 1515Z, 1545Z, 2145Z IR and 2145Z VIS are archived for EDS.

4. DESCRIPTION OF THE STUDY AREA

The region selected for the insolation test is bounded by the 29°N and 49° N parallels of latitude and the 95°W and 105°W meridians. This geographic block with dimensions of 10° longitude by 20° latitude covers an area of about 1,560,000 square km. The area (figure 1) includes the bulk of the Great Plains and is comprised of all or parts of 13 states: Minnesota, Iowa, Missouri, North Dakota, South Dakota, Nebraska, Kansas, Oklahoma, Texas, Montana, Wyoming, Colorado, and New Mexico.

According to the U.S. Geological Survey (USGS 1970), the region is comprised of over 75 percent farmland with wheat, sorghum, and barley being the predominant crops. Mean annual precipitation ranges from 30 cm in the western

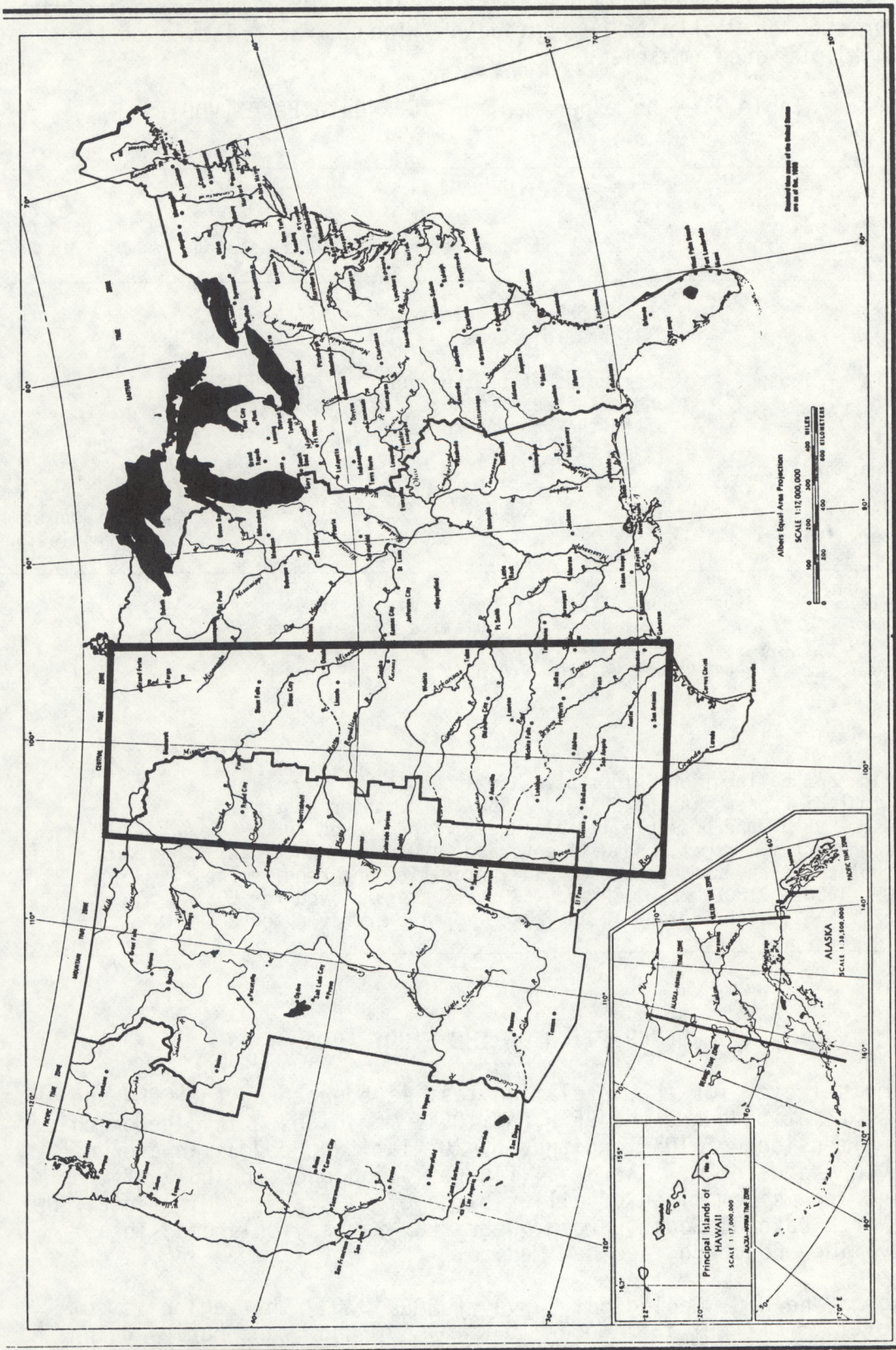


Figure 1.--Area covered by surface insolation experiment.

Dakotas up to 100 cm in eastern Oklahoma and Texas. Daily temperatures for the June, July, and August test period average about 26°C with daily maximums averaging 5°C higher. The area is classified by the USGS as "marginal" regarding drought potential; that is, it is vulnerable to droughts of long duration.

Elevation above sea level in the test area rises continuously from about 300 m in the east to 1,600 m in the west. Land-surface forms vary from the broad, flat Red River of the north plain along the Minnesota-North Dakota border to the domed Black Hills of South Dakota where elevations peak at over 2,100 m.

Most of the test area is displayed in figure 2, a 1-km resolution image transmitted by GOES-1 on September 30, 1976, at 1800Z (local noon). A number of surface landmarks in the test area are annotated including three large reservoirs formed by dams on the Missouri River: Oahe in South Dakota, Garrison in North Dakota, and Ft. Peck in Montana. Owing to the thick cover of ponderosa pine forests, the Black Hills of South Dakota show up as the darkest (least reflective) feature on the image. Southeast of the Black Hills are the barren, weathered rock formations of the Badlands, the lightest (most reflective) surface feature on the image. Barely visible in western Nebraska is Lake McConaughy, formed by a dam on the North Platte River constructed several miles upstream from its confluence with the South Platte. Numerous small reservoirs can also be seen dotting the Oklahoma-Texas region. The largest of these, Lake Texoma, is the product of a Red River dam on the Texas-Oklahoma border. The forested ranges of the Rocky Mountains are clearly visible on the left-hand side of the image.

5. SATELLITE AND CONVENTIONAL METEOROLOGICAL DATA COLLECTION

Visible solar radiation incident on the Earth is either reflected to space, absorbed in the atmosphere, or absorbed by the Earth's surface. Surface insolation, the quantity of interest, is a function of incident solar radiation and the amounts of energy reflected to space and absorbed in the atmosphere.

The visible solar radiation flux incident at the top of the atmosphere is precisely known; it is a function of solar zenith angle and Sun-Earth distance. It is depleted in a clear atmosphere by absorption and scattering, resulting in an attenuated direct beam and a significant flux of diffuse radiation. The major absorbers are water vapor and aerosols. Radiation is scattered by atmospheric molecules (Rayleigh scattering) and aerosols (Mie scattering). In the presence of clouds, there is a very large increase in scattering and some increase in absorption, and, of course, less incoming radiation at the surface.

It is not known what quantities measurable from satellites and/or obtainable from NMC are the best predictors of surface insolation. The quantities obtained for this experiment were surface pressure and precipitable water from NMC and mean target brightness, cloud amount, and cloud brightness from satellite observations.

1800 30SE76 13A-H 01831 12491 DA39N100W-2

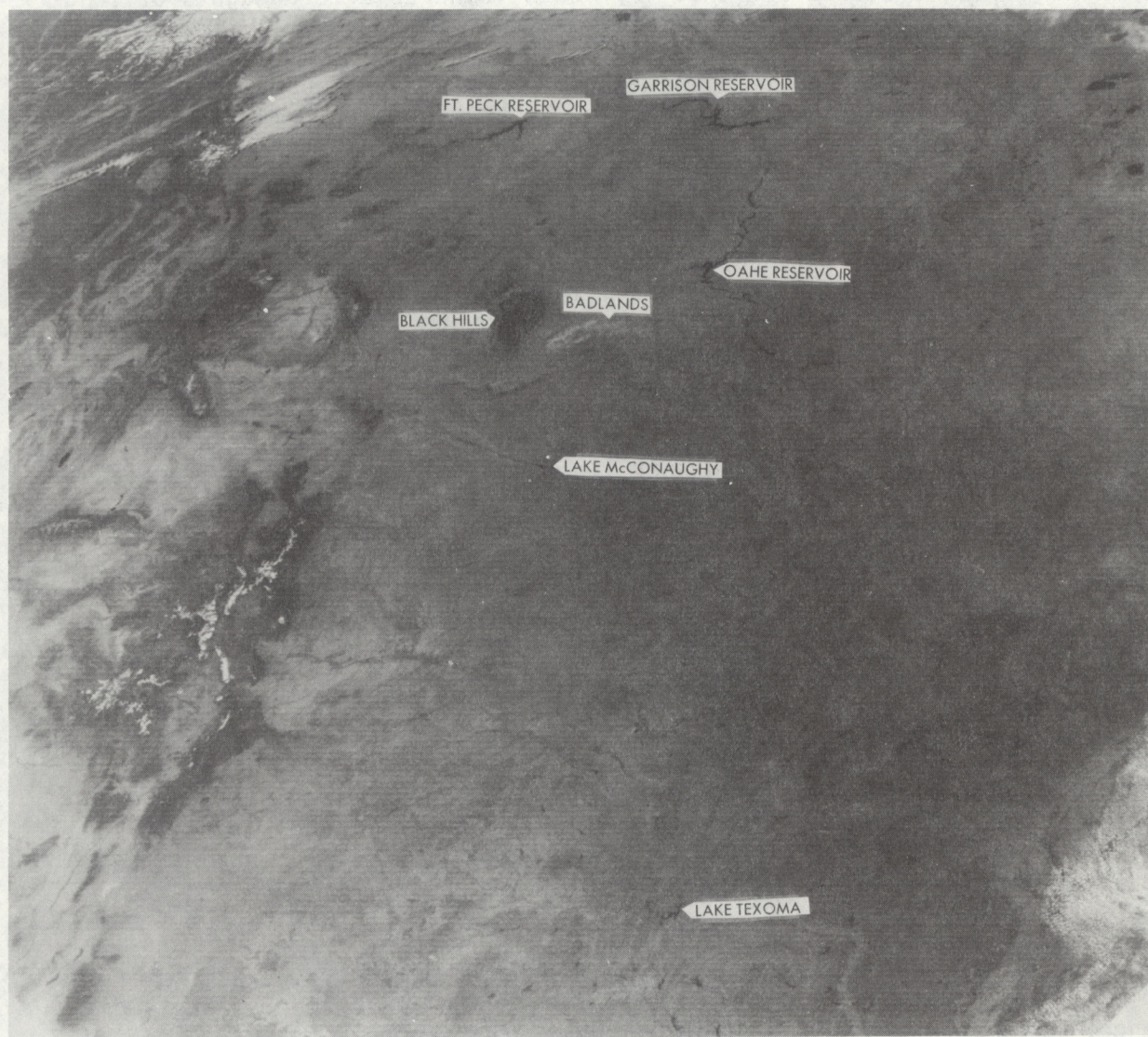


Figure 2.--One-km GOES-1/VISSR image taken over the test area on September 30, 1977.

Surface pressure is a measure of the total air mass traversed by the radiation and should be correlated with the depletion caused by molecular scattering. Precipitable water (the total water in an atmospheric column) provides information on absorption and scattering by water vapor.

The three satellite-derived quantities describe cloud conditions and total scattered radiation from the targets. The mean target brightness measures the reflected radiation due to all causes; the cloud amount and brightness yield information on the radiation component absorbed and scattered by clouds.

For the experiment, the Great Plains was divided into targets that were approximately 50 km on a side, made up of 7x6 arrays of pixels. The targets were centered at the intersections of $1/2^\circ$ -interval latitude and longitude lines beginning at the study area boundaries. Thus, the Great Plains was divided into 861 targets in a 21x41 array. Data were collected for each target.

5.1. Determination of Target Clear Radiances

To determine cloud characteristics, it was necessary to know when each pixel was cloud free. The approach used here was to compute an expected clear-radiance count value for each target on the basis of solar zenith angle and the azimuth angle between the Sun and satellite. Regression techniques with coefficients derived from a set of clear observations were used to estimate clear radiances.

5.1.1. Data Collection

To compute clear-radiance regression coefficients, a set of more than a hundred observations per target was collected and stored. Clear radiances were calculated on a 2° grid, and values of $1/2^\circ$ target intervals were achieved by interpolating between grid points. The 2° grid provided clear radiances at high enough resolution to account for most topography- and vegetation-caused variations in the Great Plains surface albedo and, at the same time, saved handling large amounts of data required by full $1/2^\circ$ resolution.

During 27 days in May 1977, data were accessed at each 2° grid point from as many visible pictures as were available for each day. The data were in arrays of 9x9 pixels centered on the grid points; the arrays were approximately 100 km on a side. These clear-radiance data arrays were larger than the insolation targets to give a more representative value when the clear radiances were interpolated at $1/2^\circ$ intervals. Quantities computed and stored for each 2° grid point were the target array mean and standard deviation and the solar azimuth and zenith angles.

5.1.2. Determination of Regression Coefficients

Processing of the data to obtain regression coefficients required the elimination of cloud-contaminated observations and fitting a regression

equation to the remaining clear cases. Figure 3 illustrates the steps in the procedure. An automatic cloud detection and elimination procedure was used because of the large volume of data.

The data were processed by target. A pass was made through the data discarding samples with solar zenith angles greater than 85° or with target standard deviation greater than 1.3 counts. Samples taken at large solar zenith angles were more likely to be anomalous, probably because of cloud shadows. Standard deviation was used as an indicator of clouds in the target; the standard deviation test threw out about 90 percent of the cloud-contaminated cases.

The data remaining after the initial sort were fitted to a regression equation of the form,

$$CR = a + b \cos \chi + c \sin \chi \cos \phi + d \sin \chi \cos^2 \phi ,$$

where CR is the visible clear radiance from the target, χ is the local solar zenith angle, and ϕ is the azimuth angle between Sun and satellite. The angles are shown in figure 4. The second term on the right of the equation accounts for changing incident flux; the last two terms account for changes in apparent target brightness caused by shadowing at the surface.

The sort on standard deviation produced a data set sufficiently cloud free that a reasonable clear-radiance prediction equation was obtained from it. Residuals from the "first-guess," clear-radiance equation were used to identify remaining cloud-contaminated data. This was a cyclic procedure (figure 3) that, after two cycles, yielded a cloud-free data set and accurate regression coefficients.

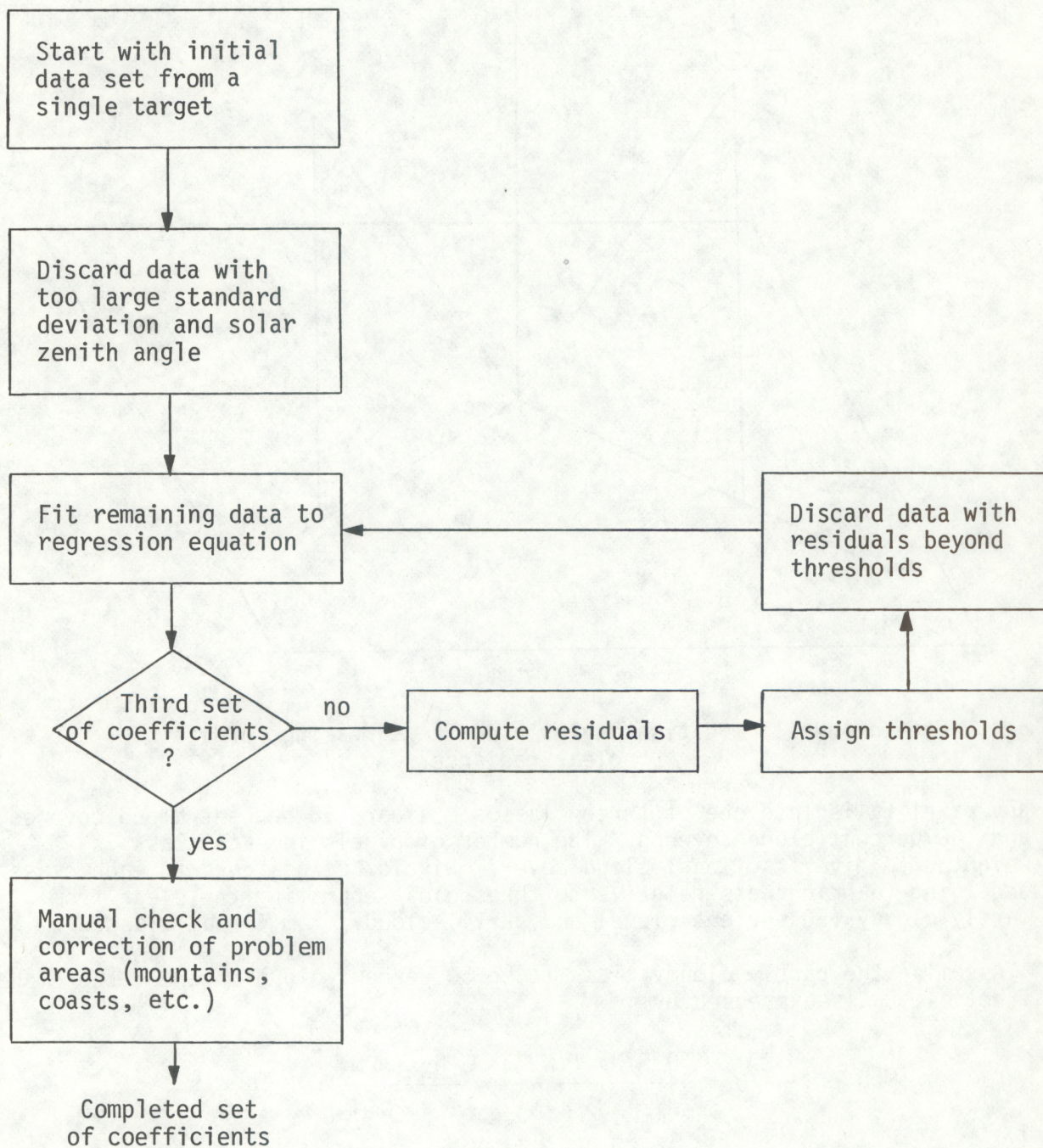
The residuals, defined as the difference between the measured and predicted radiances, were compared against thresholds; residuals exceeding these thresholds were discarded from the data set. The thresholds were tightened between the first and second passes through the data to eliminate data contaminated by small amounts of cloudiness.

The standard error of the estimate for the final regression equation ranged from 0.5 to 0.9 counts for most Great Plains' targets, an accuracy considered sufficient for assigning clear/cloudy thresholds. Targets containing features with markedly contrasting brightness could not be accurately fitted to the regression equation. Such targets included those containing mountain ranges, coastal areas, and large lakes. In all these cases, the regression coefficients determined for targets with a uniform surface as bright as the brightest feature in the nearest nonuniform target were used to predict clear radiance for the nonuniform target. This procedure insured that no clear surface was mistaken for cloudiness in the nonuniform targets. The regression coefficients used for each 2° grid point are given in appendix A.

5.2. Cloud Amount

Cloud amount in each target was computed using a two-threshold method (Shenk and Salomonson 1972). The approximation basic to this method is that

Figure 3.--Procedure for obtaining clear-radiance coefficients for a specific target.



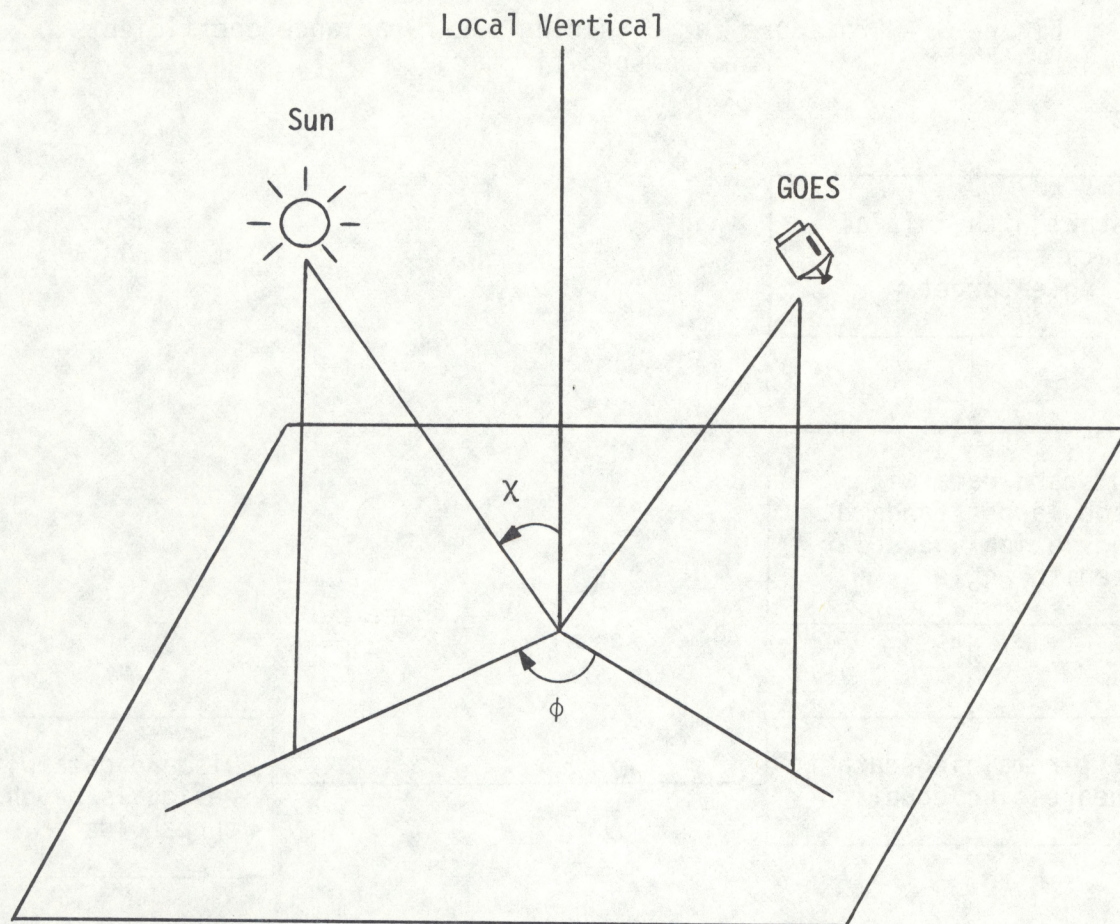


Figure 4.--Illumination angles used in regressing for visible clear radiance.

any pixel falls into one of three classes: clear, 50 percent cloud covered, and 100 percent cloud covered. The number of pixels in each class is weighted to give fractional cloud cover. Pixels are assigned to each class according to brightness relative to thresholds separating the clear from partly-cloudy (50 percent cloud) and partly-cloudy from cloudy classes.

Assuming the partly cloudy class to be 50 percent cloud covered, the cloud fraction, C , is expressed by

$$C = \frac{0.5 N_2 + N_3}{N_1 + N_2 + N_3} = \frac{N_2 + 2N_3}{2N} ,$$

where N is the total number of pixels in the target area and N_1 , N_2 , and N_3 are the numbers of pixels in the clear, partly-cloudy, and cloudy classes, respectively.

A clear/partly-cloudy threshold, T_1 , was obtained by adding three counts to the clear radiance predicted by regression. A pixel was called clear if its

count value was $\leq T_1$. A partly-cloudy/cloudy threshold, T_2 , was taken to be the clear radiance plus five counts. The partly-cloudy pixels were those with values $> T_1$ and $\leq T_2$. The cloudy pixels were those $> T_2$.

The accuracy of the cloud fraction algorithm is unknown. The thresholds used were set to yield relatively good estimates with bright waterdrop clouds. (Thin cirrus clouds in the target lead to underestimates of cloud amount.) For inferring insolation, it is probably sufficient to have a quantity that is a sensitive indicator of cloud cover; it is not necessary that it be absolutely accurate.

5.3. Computation of Cloud Brightness

The amount of solar radiation absorbed and reflected by clouds is a function of cloud thickness. The brightness of clouds when observed from a satellite is a good indicator of their thickness, so mean cloud brightness was included in the insolation data set. Mean cloud brightness was computed by averaging the count values of all pixels in a target that were brighter than the partly-cloudy/cloudy threshold. If there were no pixels brighter than the threshold, then the brightness was set to zero.

5.4. Mean Target Brightness

The third satellite-derived quantity computed for each target was the mean brightness. This quantity is simply the mean count value of all pixels in each 7x6 pixel array (target).

5.5. Precipitable Water and Surface Pressure

Two readily available meteorological quantities that affect the amount of solar radiation reaching the surface are atmospheric pressure and moisture. These quantities were accessed from the NMC 00Z data file in the form of surface pressure (mb) and precipitable water (mm/cm^2). These files are updated twice daily; the 00Z file contains information most nearly time-coincident with the satellite measurements. The data are kept in the NESS/NMC computing facility on a 65x65 mapped data array. Accessing routines retrieve pressure and precipitable water for each target using the values at the nearest NMC grid point which, in the Great Plains region, may be as far as 2° latitude and longitude from the target.

5.6. Calculation of Solar Zenith and Azimuth Angles

Hourly values of local solar zenith and azimuth angles used to compute expected clear radiances (figure 4) were saved for each target for possible use in analyzing the data. Computation of azimuth and zenith angles requires the latitude and longitude of the target, solar declination, and time of observation. Latitude and longitude can be exactly specified. The solar declination changes slowly, especially during the summer, so the value used was the declination of 1200 GMT on the day of the observation.

The beginning time for each picture from the east satellite is on the hour and half hour. The instrument scans the Great Plains between five and ten minutes after initiation of the picture; however, the exact measurement time

for each target is unknown. The beginning time was used for computation of the solar position angles. The resulting errors were in the neighborhood of one degree.

6. RESULTS OF SUMMER 1977 COLLECTION EFFORT

The GOES-1, 8-km VDB was used between June 1 and August 15 to extract information from about 10 pictures daily (1400, 1500, 1600, 1700, 1800, 2000, 2100, 2130, 2200, and 2300Z). The 1900Z time slot was reserved for production of 1-km sectors over the Western United States and, thus, was not available to the VDB.

Sixty-three days of usable data were obtained during the 75-day test; the 12 "bad" days are accounted for in table 2. The 63 days of usable data translated into 630 possible time slots or pictures available for the study. The 630 time slots resulted in 485 usable pictures, 35 unusable pictures, and 110 missing pictures. Unusable pictures account for only 6.77 percent of the total pictures received. Unusable pictures included those caused by excess line dropout, mislocation, and bad data. Of the 35 unusable pictures, 15 were received during a one-week satellite transition period (August 7-14, 1977); data on most of the unusable pictures were not properly geographically registered.

Table 2.--Breakdown of lost days of data

Reasons	Date	Number of days lost
User program error-cloud subroutine	June 1-6	6
User program error-line limits	June 10-11	2
Unavailability of NMC data base	June 8	1
Output disk file not mounted by operator*	July 2	1
Unintelligible output	July 8	1
Data lost in transfer from disk to tape	July 27	1
Total		12

*Output file switched to an on-line disk starting on this date.

As can be seen in table 3, the total number of usable pictures was 485. Of these, 80 pictures contained some line dropout. The 485 usable pictures, when averaged over 63 days, yielded 7.65 pictures per day. A histogram showing the daily number of usable pictures over the entire period is given in figure 5.

Throughout the test period, one designated target was monitored twice daily to check the accuracy of scene brightness values derived from the clear-radiance regression. The target, located in east-central Kansas at 38°N, 97°W, is fairly representative of the test area. Comparisons of the measured versus the predicted responses at 1600Z and 2100Z are shown respectively in

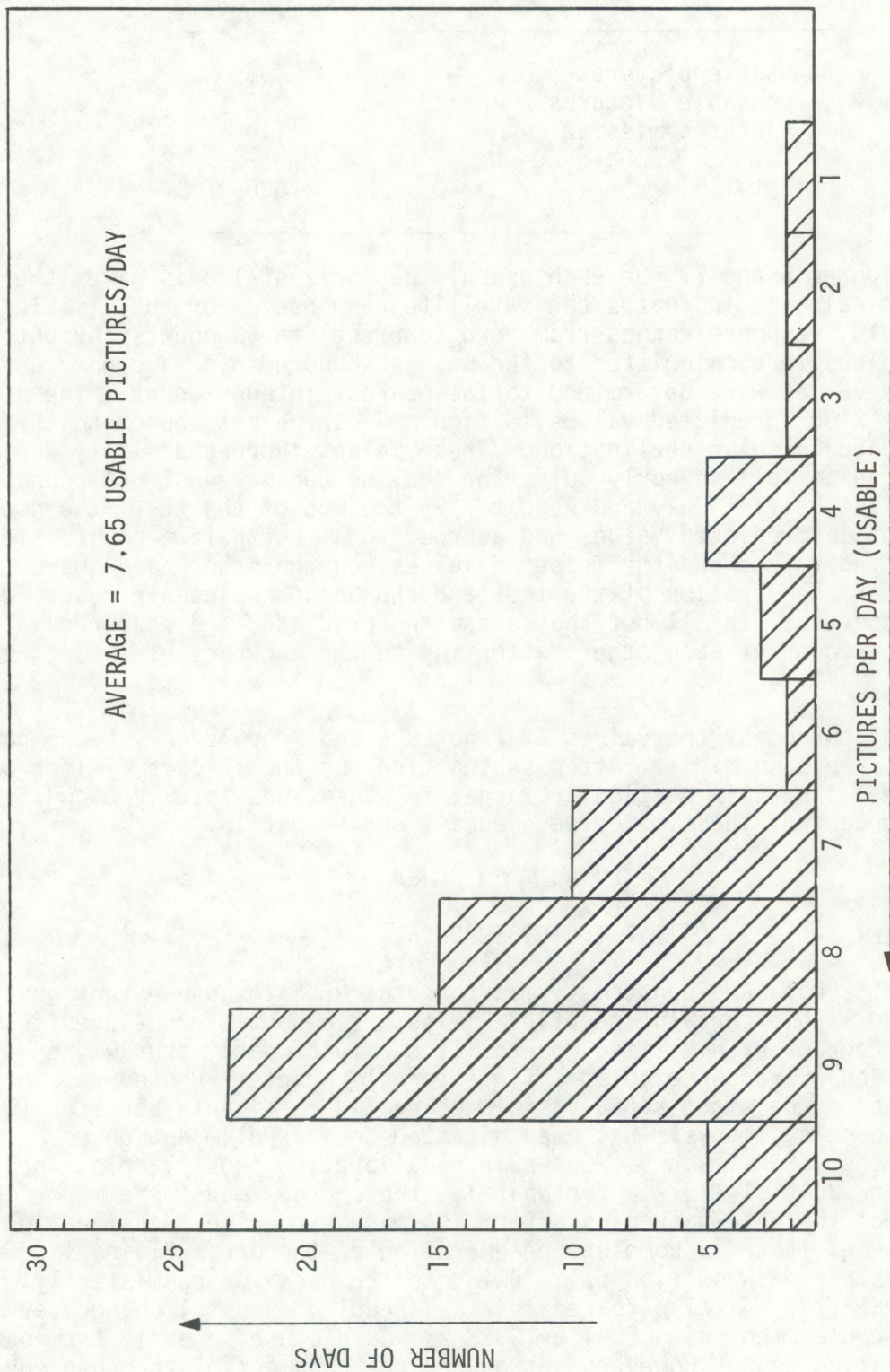


Figure 5.--Histogram showing the daily number of pictures successfully utilized during the test period.

Table 3.--Breakdown of possible time slots

Usable pictures	485
Unusable pictures	35
Pictures missing	<u>110</u>
Total	630

graphs on figures 6 and 7. On each graph, the horizontal axis gives the date and the vertical axis indicates the satellite response. For the visible VISSR channels, response ranges from zero (darkest) to 63 counts (brightest). Predicted values were calculated to the nearest hundredth of a count, and the measured values were determined to the nearest integer count. The variation of 2100Z predicted values in figure 7 can be attributed to the seasonal change in solar declination. These values increased slowly during June but began to fall in early July; the decline became even more pronounced during the last half of July and August. By the end of the test, the downward movement in predicted values had accrued to almost half a count. The 1600Z predicted values and the measured values, on the other hand, were consistent for the duration of the test and showed no noticeable change with season or land use. In all but two cases, the predicted and measured values were within a count of each other, attesting to the accuracy of the regression model.

For control purposes, the values of figures 6 and 7 could only be compared under cloud-free conditions. After subtracting out the 12 days of lost data, it can be seen that this particular target in Kansas was totally cloud free almost 50 percent of the time between June 1 and August 15.

7. QUALITY CONTROL

7.1. VISSR Data

The raw VISSR data are constantly monitored at NESS to assure that quality is maintained within certain specified limits. Diagnostic procedures include checking histograms of digitized counts, linearity of data, step wedge values, and sensor response to specific external targets. Procedures for normalization of the eight VISSR visible channels are given by Bristor (1975). For these channels, emphasis has been directed towards elimination of striping in the VISSR imagery. One such recalibration took place during the test period on July 21, 1977. Fortunately, the changes made were minor and did not affect the data-gathering effort. A more extensive recalibration might have necessitated a complete regeneration of the Great Plains land-use data base described in section 5.1. Owing to the need for consistently calibrated data, it was also feared that a scheduled August 1 changeover of satellites (replacement of GOES-1 by GOES-2) would cause an early termination of the insolation test. However, a two-week postponement of the changeover was granted to allow the insolation test to run to completion.

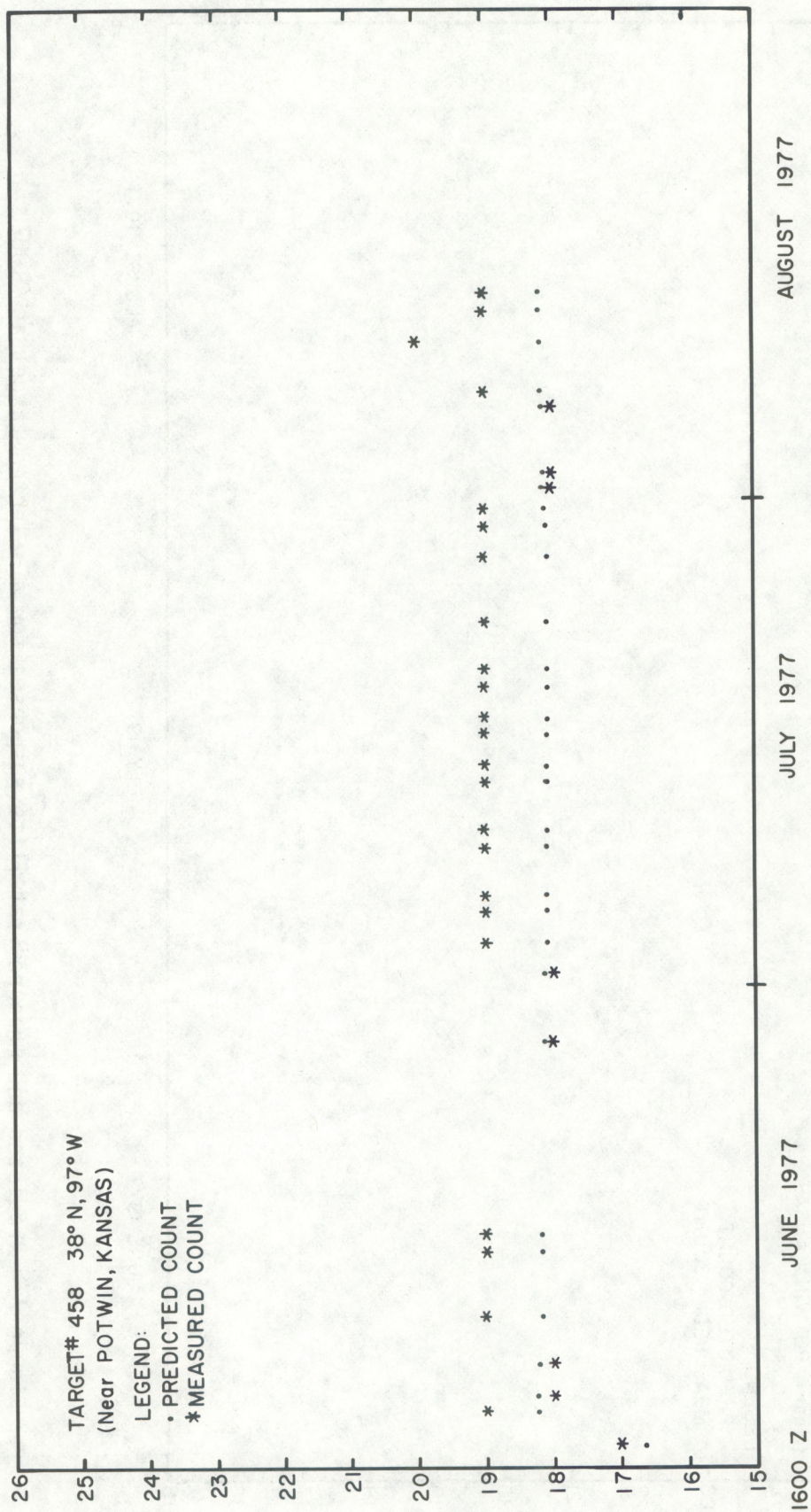


Figure 6.--Predicted and measured satellite responses for a selected target at 1600Z.

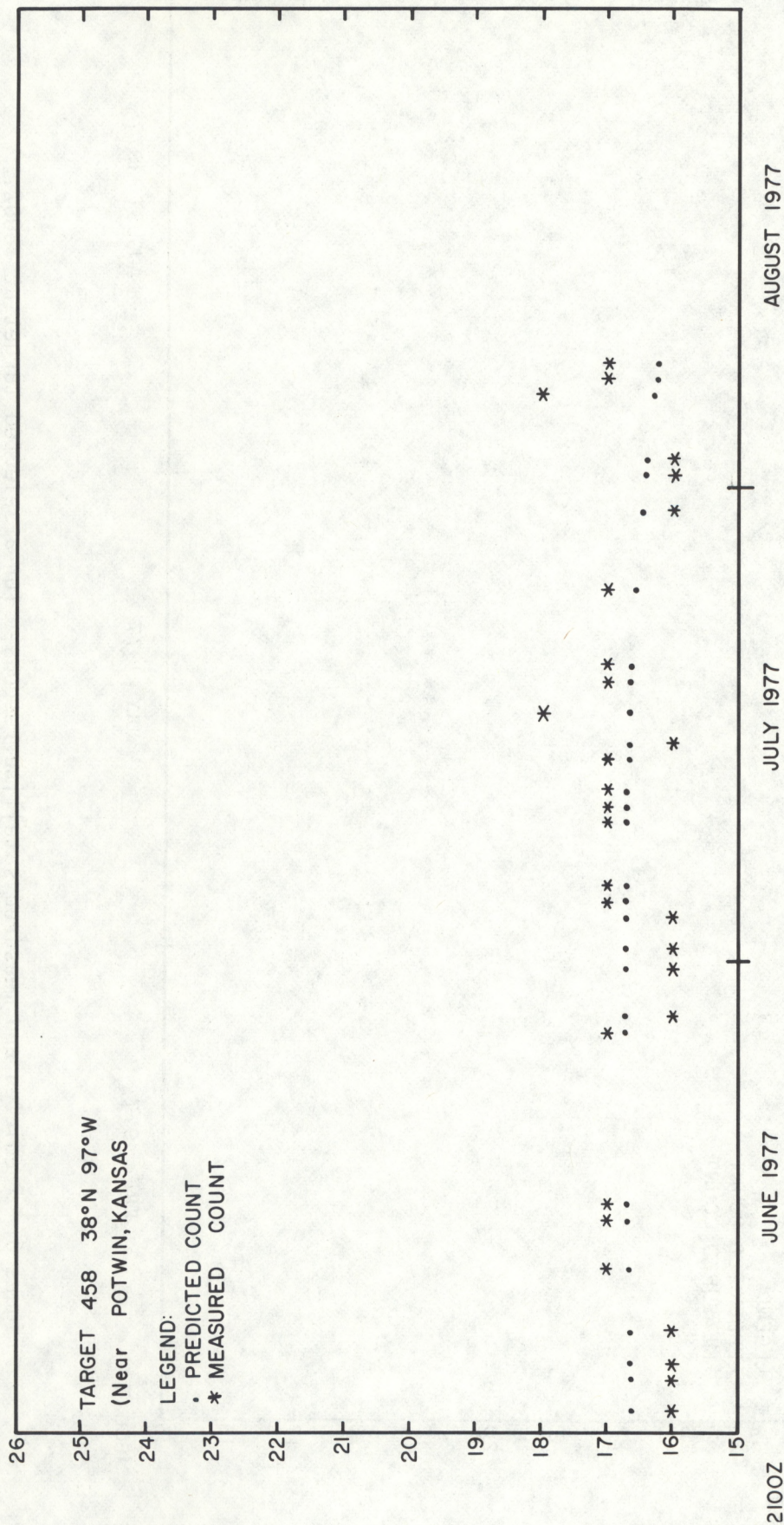


Figure 7.--Predicted and measured satellite responses for a selected target at 2100Z.

7.2. Test Data

The collected data were printed out daily so that values could be checked and geographic registration verified. Line dropout and invalid data were noted using both automatic and manual techniques. Brightness values, not in the valid 0-to-63 range, were tagged with a "-1" and their location was recorded in a log book.

Earth location was checked through the use of alphanumeric printouts giving a representation of each picture accessed from the VDB. Such a printout (reduced in scale) is displayed in figure 8. The printout is composed of alphanumeric characters, each character representing a pixel of 8-km resolution. Look-up tables were devised to assign the alphanumeric characters to the visible count values in such a way as to give a representation of surface features and clouds. The 10 characters used (WX0&=+,-,. and blank) are arranged so that W's correspond to the lowest (darkest) values and blanks correspond to the highest (brightest) values. Thus, bodies of water are represented by a field of W's in the printout and clouds appear as blank. The look-up tables were varied with time of day to accommodate hourly changes in tone and contrast. Separate tables were used for the following time periods: 1400 and 2300Z, 1500 and 2200Z, 1600 and 2100Z, and 1700 through 2000Z.

The printout in figure 8 depicts the Great Plains at 1600Z on April 25, 1977. It contains 286 scan lines and is bounded by the 49°N parallel on top and the 24°N parallel on bottom. The GOES compatible grid was overlaid on the data through the use of an optical instrument, the Bausch and Lomb Zoom Transfer Scope. Particularly noticeable surface features on the printout are the Gulf Coast, Ft. Peck Reservoir in Montana, Garrison Reservoir in North Dakota, the Black Hills and Oahe Reservoir in South Dakota, Lake McConaughy in Nebraska, and Lake Texoma on the Texas-Oklahoma border. The most prominent landmark on the printout, the Black Hills, covers over 50 pixels; the smallest discernible, Lake McConaughy, covers only three. The range of count values for cloud-free targets is only six. The darkest feature, the Black Hills, is represented by an "&", which, at 1600Z, yields a count value of 17. The lightest land feature, the Badlands, is just to the southeast of the Black Hills and is represented by a swath of periods, ".", which corresponds to a count value of 23.

Any land feature can be used to verify the registration of the pictures on the VDB by comparing its location on the printout to its known geographic location. When all land features are obscured by cloud cover, a 4-km resolution GOES-1 image (figure 9) corresponding to the printout can be used for earth-location purposes. As can be seen in figure 9, there are scattered clouds just south of the Texas Panhandle and in the Oklahoma-Kansas region. These same clouds can be discerned as blank areas on the computer printout in figure 8. Similarly, mountain snowpacks and orographic clouds in Wyoming and Colorado can be seen in both image and printout.

8. DATA TAPE FORMAT

The data collection program was run once daily accessing all pictures on the VDB between 1400 and 2300Z as well as the NMC data files. The output

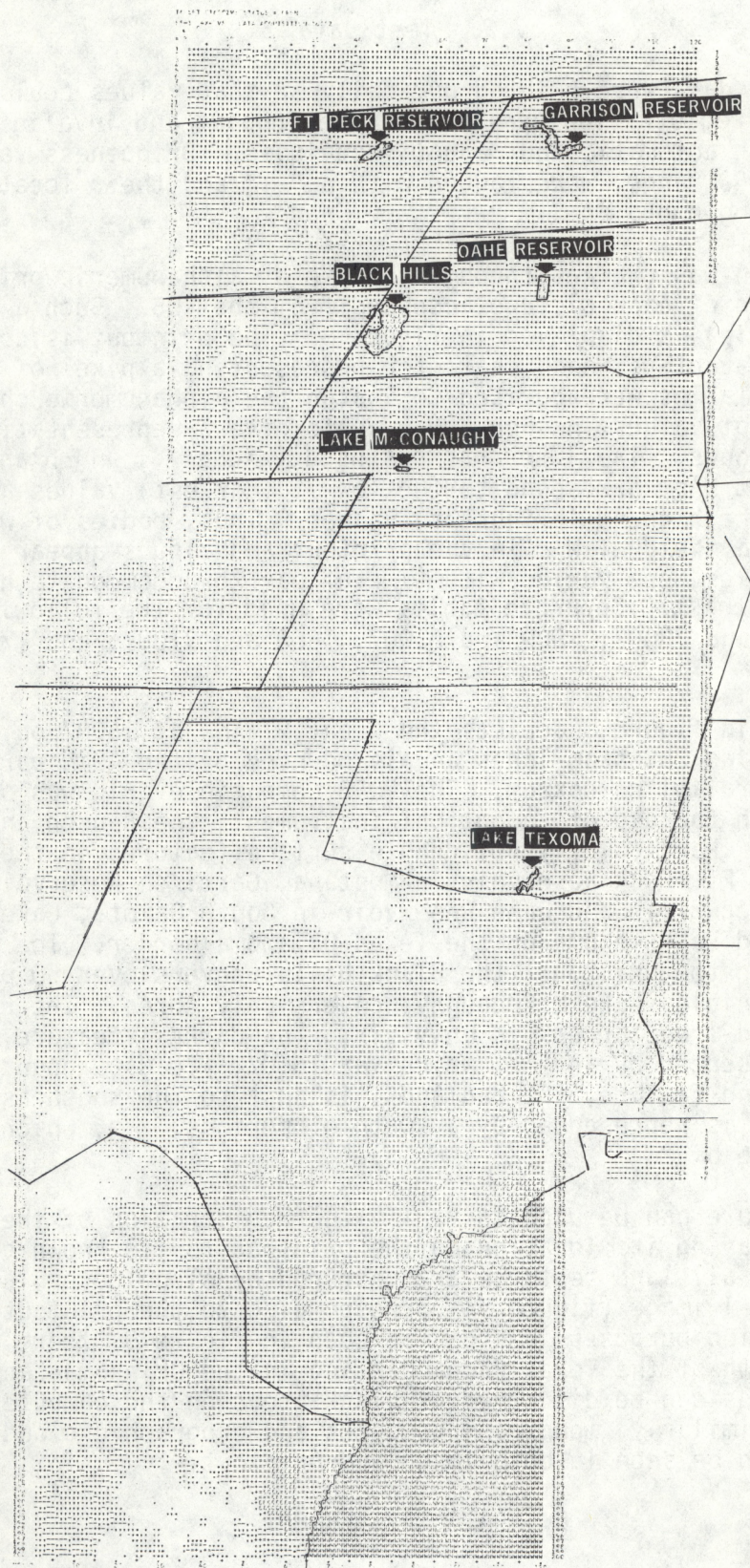


Figure 8.--Computer printout of a 1600Z VISSR image on April 25, 1977. Each character represents an 8-km pixel.

U.S. CLOUD COVER
25 APRIL 1977 1700 GMT
NOAA SATELLITE PHOTOGRAPH
NATIONAL ENVIRONMENTAL SATELLITE SERVICE

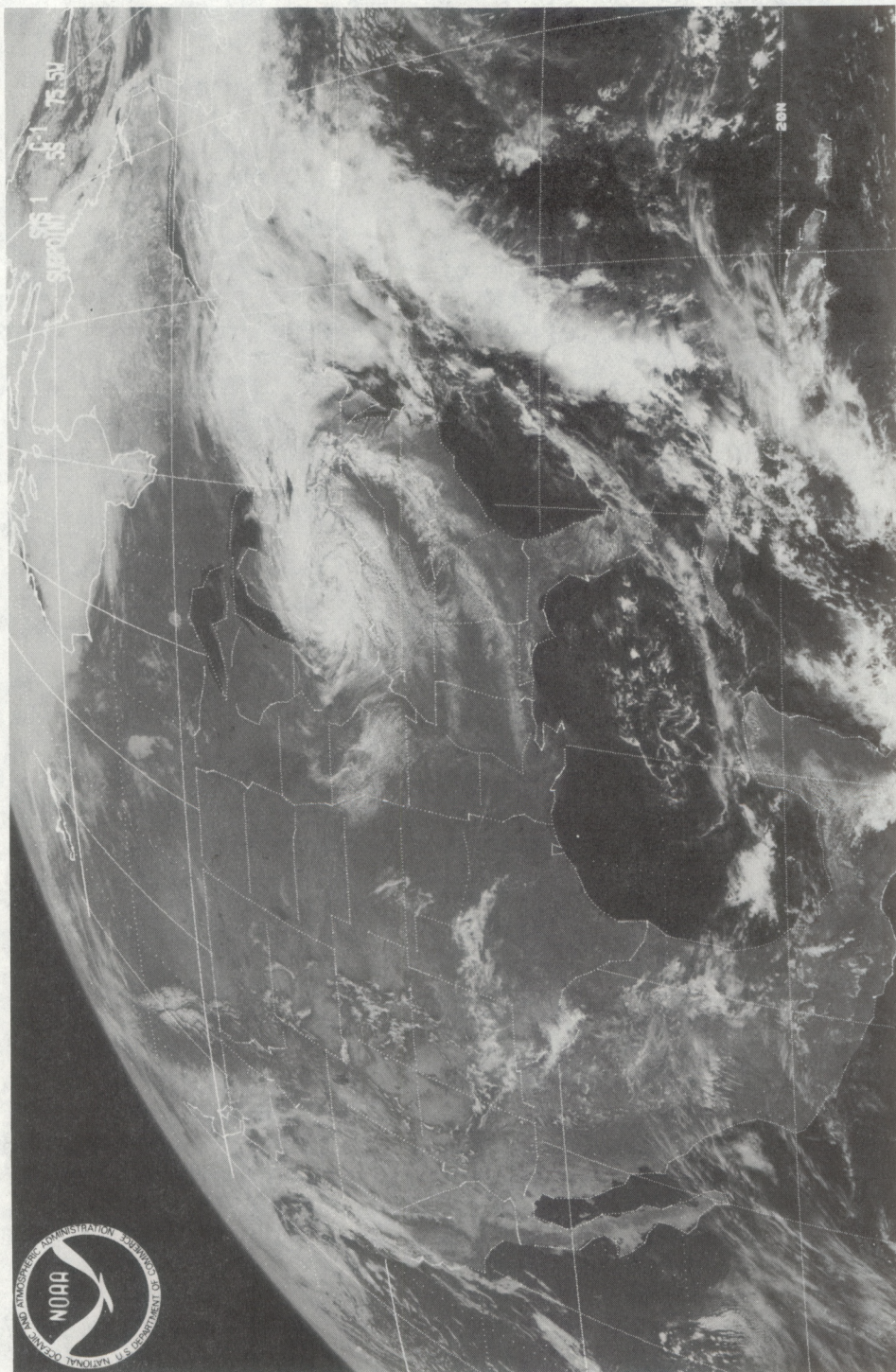


Figure 9.--A 4-km resolution VISSR image used for data registration.

data were written onto a disk pack for temporary storage and transferred each week to a nine-track, 1600 bpi magnetic tape. At the conclusion of the test, the tape contained 485 usable pictures collected over a 63-day period; all unusable pictures were deleted. Appendix B gives the date and time of each block of test data resident on the tape.

The tape consists of one file with 2,551 record blocks. Each block consists of two records:

1. Header record, 42-byte title, with a 21A2 format
 - a. quantity measured
 - b. date of data and/or time of picture
2. Data record, 1,722 bytes, with an INTEGER*2 format
 - a. 861 targets in 2-byte words
 - b. Targets are ordered starting at the northwest corner of the study area and progress from west to east and north to south, respectively.

There are seven types of data records on the tape.

1. surface pressure--millibars
2. precipitable water--millimeters
3. mean target brightness--counts
4. cloud amount--percent
5. cloud brightness--counts
6. solar zenith angle--radians times 1,000
7. solar azimuth angle--radians times 1,000

Data record types 1 and 2 (surface pressure and precipitable water) appear only at the beginning of each day; data record types 3 and 7 are present for each picture. Examples of each record type are given in appendix C.

Copies of the tape are available at a nominal price to cover cost of the tape and reproduction.

9. PYRANOMETER DATA

Much of the value of the satellite data set is due to the coincident ground-truth measurements made with the GPC pyranometer network. The network consists of about 40 pyranometers well distributed over the Great Plains. The sensors measured hourly integrated radiation with the hour beginning and ending on the half hour. The instruments were calibrated to a single standard; calibrations were made in early August near the end of the observing period.

The pyranometers ran from June 1, 1977, through August 31, 1977. The data were collected, quality checked, and stored on magnetic tape at the Blackland Research Center at Temple, Texas.

10. SUMMARY

The purpose of the summer 1977 effort was to collect a coincident set of pyranometer, satellite, and conventional meteorological data for the study of satellite-inferred insolation. This report details the collection of the satellite and meteorological parts of the data and provides a set of regression coefficients for use in determining clear radiance. The relationships between pyranometer and satellite data are being studied by NESS and GPC investigators. The authors urge interested persons or organizations to compare these data and examine the merits of satellite data for the measurement of insolation.

The satellite and conventional meteorological data sets can be obtained from

Mr. J. Emmett Bragg
Environmental Products Group, S132
NESS, World Weather Building
5200 Auth Road
Camp Springs, Maryland 20233

Information on the pyranometer data set is available from

Dr. J.T. Ritchie
USDA-ARS Blackland Research Center
P.O. Box 748
Temple, Texas 76501

ACKNOWLEDGMENTS

The authors would like to thank Leo V. Strees and David F. McGinnis, Jr., of the NESS/Environmental Sciences Group for development of solar declination and equation-of-time subroutines used in this model; Robert M. Carey of the NESS/Applications Division for programming assistance on the clear-radiance procedures; and Martha Young of NESS/Applications Division for assistance with the figures.

REFERENCES

- Bristor, C.L., 1975: Central processing and analysis of geostationary satellite data. NOAA Technical Memorandum NESS 64, National Oceanic and Atmospheric Administration, U.S. Department of Commerce, Washington, D.C., 155 pp.
- Shenk, W.E. and V.V. Salomonson, 1972: A simulation study exploring the effects of sensor spatial resolution on estimates of cloud cover from satellites. Journal of Applied Meteorology, 11, 214.
- U.S. Geological Survey, 1970: The national atlas of the United States of America. U.S. Department of Interior, Washington, D.C., 417 pp.

Mention of a commercial company or product does not constitute an endorsement by the NOAA National Environmental Satellite Service. Use for publicity or advertising purposes of information from this publication concerning proprietary products or the tests of such products is not authorized.

APPENDIX A. REGRESSION COEFFICIENTS FOR PREDICTING CLEAR RADIANCE

LAT	LONG	a	b	c	d
49	105	9.57	11.49	1.25	4.78
49	103	9.54	10.78	1.22	4.56
49	101	9.95	9.38	.38	4.98
49	99	8.93	9.80	.76	4.43
49	97	9.68	8.66	1.81	2.50
49	95	9.68	8.66	1.81	2.50
47	105	8.26	12.40	1.93	4.86
47	103	8.91	10.76	1.18	4.98
47	101	9.19	9.96	.80	4.47
47	99	8.31	10.45	1.76	3.84
47	97	8.58	8.79	1.21	3.84
47	95	8.25	9.58	1.39	2.83
45	105	8.03	11.18	1.57	5.20
45	103	9.07	10.89	1.52	4.32
45	101	9.33	9.80	2.02	3.93
45	99	8.57	9.81	1.40	4.07
45	97	8.07	10.29	.40	4.12
45	95	7.35	10.85	1.44	2.06
43	105	8.29	12.82	.03	6.11
43	103	7.77	11.87	1.19	4.80
43	101	8.34	11.56	1.38	4.57
43	99	8.66	9.78	.94	4.07
43	97	7.91	10.43	.11	4.81
43	95	7.12	9.89	1.02	3.35
41	105	7.71	12.31	.88	5.45
41	103	7.71	12.31	.88	5.45
41	101	7.60	12.69	1.07	5.42
41	99	8.33	12.18	.73	4.73
41	97	7.56	11.55	1.56	3.67
41	95	7.88	10.42	1.75	3.66
39	105	6.91	14.39	.92	5.42
39	103	6.91	14.39	.92	5.42
39	101	7.67	12.22	.59	4.84
39	99	8.45	10.45	.04	5.34
39	97	8.05	10.36	.78	3.80
39	95	9.42	8.43	1.27	2.85
37	105	5.86	14.63	1.10	7.71
37	103	5.86	14.63	1.10	7.71
37	101	7.61	14.05	.82	4.68
37	99	7.69	11.38	.73	4.86
37	97	8.87	9.08	.79	3.38
37	95	7.95	10.08	.71	4.13
35	105	4.94	15.43	2.58	4.72
35	103	5.62	15.35	2.11	5.20
35	101	6.48	13.02	.68	5.52
35	99	7.72	10.68	.95	4.58
35	97	7.33	10.56	1.04	4.47

LAT	LONG	a	b	c	d
35	95	7.38	9.98	0.39	5.30
33	105	4.88	15.73	2.12	6.82
33	103	4.88	15.73	2.12	6.82
33	101	5.84	13.12	.92	6.66
33	99	7.00	11.45	.65	5.13
33	97	8.23	9.95	1.05	3.96
33	95	7.53	9.41	1.33	4.69
31	105	3.02	18.71	3.80	6.81
31	103	4.48	19.25	2.45	5.94
31	101	5.58	12.83	1.18	5.56
31	99	5.26	12.72	.82	6.22
31	97	7.39	10.59	.56	4.80
31	95	7.57	11.37	2.40	-2.72
29	105	2.38	19.30	4.39	5.98
29	103	3.93	16.88	1.54	7.63
29	101	5.01	13.95	1.43	5.25
29	99	6.06	11.38	1.30	4.84
29	97	6.20	11.00	1.97	4.44
29	95	7.57	11.37	2.40	-2.72

APPENDIX B. DATE AND TIME OF PICTURES

Date		Time (Z)					Total number of pictures
1	6-07-77	1600	1800	2000	2100	2130	7
		2200	2300				
2	6-09-77	1400	1500	1600	1700	2000	9
		2100	2130	2200	2300		
3	6-12-77	1500	1600	1700	1800	2000	9
		2100	2130	2200	2300		
4	6-13-77	1600	1700	1800	2000	2100	8
		2130	2200	2300			
5	6-14-77	1400	1600	1700	1800	2000	9
		2100	2130	2200	2300		
6	6-15-77	1500	1600	1700	1800	2000	9
		2100	2130	2200	2300		
7	6-16-77	1400	1600	1700	1800	2000	8
		2100	2130	2200			
8	6-17-77	1400	1500	1600	1700	2000	9
		2100	2130	2200	2300		
9	6-18-77	1500	1600	1700	1800	2000	8
		2100	2130	2200			
10	6-19-77	1400	1500	1600	1800	2000	9
		2100	2130	2200	2300		
11	6-20-77	1500	1600	1700	1800	2000	9
		2100	2130	2200	2300		
12	6-21-77	1400	1500	1600	1700	1800	10
		2000	2100	2130	2200	2300	
13	6-22-77	1400	1500	1600	2000	2100	8
		2130	2200	2300			
14	6-23-77	1600	1700	2000	2100	2130	7
		2200	2300				
15	6-24-77	1600	1700	1800	2000	2100	8
		2130	2200	2300			

Date		Time (Z)					Total number of pictures
16	6-25-77	1400	1500	1600	1700	1800 2000 2100 2130 2200 2300	10
17	6-26-77	1400	1500	1600	1700	1800 2000 2100 2130 2200 2300	10
18	6-27-77	1500	1600	1700	1800	2000 2100 2130 2200	8
19	6-28-77	1400	1500	1600	1700	1800 2000 2130 2200 2300	9
20	6-29-77	1400	1500	1600	1700	1800 2130 2200 2300	8
21	6-30-77	1600	1700	2000	2100	2130 2200 2300	7
22	7-01-77	1400	1500	1600	1800	2100 2130 2200 2300	8
23	7-03-77	1400	1500	1600	1700	1800 2000 2100 2200 2300	9
24	7-04-77	1400	1500	1700	2000	2100 2200 2300	7
25	7-05-77	1500	1600	1700	1800	2000 2100 2130 2200 2300	9
26	7-06-77	1500	1600	2000			3
27	7-07-77	1500	1700	1800	2100	2130	5
28	7-09-77	1500	1600	1700	2000	2100 2200 2300	7
29	7-10-77	1400	1500	1600	1700	2000 2100 2130 2200 2300	9
30	7-11-77	1600	1700	1800	2000	2100 2130 2200 2300	8
31	7-12-77	1400	1600	1700	2000	2100 2130 2200	7
32	7-13-77	1500	1600	1800	2000	2100 2130 2200 2300	8

	Date	Time (Z)	Total number of pictures
33	7-14-77	1400 1500 1600 1700 1800 2000 2100 2300	8
34	7-15-77	1600 1800 2000 2100 2130 2200 2300	7
35	7-16-77	1400 1500 1600 1700 1800 2000 2100 2200 2300	9
36	7-17-77	1400 1500 1600 1700 2000 2100 2130 2200 2300	9
37	7-18-77	1600 1700 1800 2000 2100 2130 2200	7
38	7-19-77	1600 1700 1800 2100 2130 2200 2300	7
39	7-20-77	1400 1500 1600 1700 1800 2000 2100 2130 2300	9
40	7-21-77	1500 1600 1700 1800 2000 2100 2130 2200 2300	9
41	7-22-77	1500 1600 1700 1800 2100 2130 2200 2300	8
42	7-23-77	1500 1600 1700 1800 2000 2100 2130 2200 2300	9
43	7-24-77	1400 1500 1600 1700 1800 2000 2100 2130 2200 2300	10
44	7-25-77	1500 1600 1700 1800 2000 2100 2130 2200 2300	9
45	7-26-77	1400 1500 1600 1800 2000 2100 2130 2200 2300	9
46	7-28-77	1400 1500 1600 2300	4
47	7-29-77	1400 1500 1600 1700 2000 2100 2130 2200 2300	9
48	7-30-77	1400 1500 1600 1800 2000 2100 2130 2200 2300	9

		Time (Z)				Total number of pictures
Date						
49	7-31-77	1400	1500	1600	1700	4
50	8-01-77	1400	1500	1600	1700 1800 2100 2130 2300	8
51	8-02-77	1400	1500	1600	1800 2100 2130 2200 2300	8
52	8-03-77	1500	1600	1800	2100 2130 2200 2300	7
53	8-04-77	1400	1500	1600	1700	4
54	8-05-77	1400	1500	1600	1700 1800 2000 2100 2130 2200 2300	10
55	8-06-77	1400	1500	1600	1700 1800 2000 2100 2130 2200	9
56	8-07-77	1400	1600	1700	1800 2000 2100 2130 2200 2300	9
57	8-08-77	1400	1600	1700	1800 2000 2100 2130 2200 2300	9
58	8-09-77	2100	2200			2
59	8-10-77	1400	1600	1700	2100 2130 2200	6
60	8-11-77	1400	1600	2100	2130 2200	5
61	8-12-77	1400	1600	1800	2300	4
62	8-13-77	1400	1600	1700	1800 2100 2130 2200 2300	8
63	8-14-77	1500				1

APPENDIX C. EXAMPLES OF EACH DATA TYPE

[illegible]

[illegible]

Data record type 7: solar azimuth angle (radians times 1,000).

(Continued from inside front cover)

- NESS 76 The Use of the Radiosonde in Deriving Temperature Soundings From the Nimbus and NOAA Satellite Data. Christopher M. Hayden, April 1976, 21 pp. (PB-256755)
- NESS 77 Algorithm for Correcting the VHRR Imagery for Geometric Distortions Due to the Earth's Curvature and Rotation. Richard Legeckis and John Pritchard, April 1976, 30 pp. (PB-258027/AS)
- NESS 78 Satellite Derived Sea-Surface Temperatures From NOAA Spacecraft. Robert L. Brower, Hilda S. Gohrband, William G. Pichel, T. L. Signore, and Charles C. Walton, June 1975, 74pp. (PB-258026/AS)
- NESS 79 Publications and Final Reports on Contracts and Grants, 1975. NESS, June 1976, 18 pp. (PB-258450/AS)
- NESS 80 Satellite Images of Lake Erie Ice: January-March 1975. Michael C. McMillan and David Forsyth, June 1976, 15 pp. (PB-258458/AS)
- NESS 81 Estimation of Daily Precipitation Over China and the USSR Using Satellite Imagery. Walton A. Follansbee, September 1976, 37 pp. (PB-261970/AS)
- NESS 82 The GOES Data Collection System Platform Address Code. Wilfred E. Mazur, Jr., October 1976, 26 pp. (PB-261968/AS)
- NESS 83 River Basin Snow Mapping at the National Environmental Satellite Service. Stanley R. Schneider, Donald R. Wiesnet, and Michael C. McMillan, November, 1976, 27 pp. (PB-263816)
- NESS 84 Winter Snow-Cover Maps of North America and Eurasia From Satellite Records, 1966-1976. Michael Matson, March 1977. (PB-267393)
- NESS 85 A Relationship Between Weakening of Tropical Cyclone Cloud Patterns and Lessening of Wind Speed. James B. Lushine, March 1977, 12 pp. (PB-267392)
- NESS 86 A Scheme for Estimating Convective Rainfall From Satellite Imagery. Roderick A. Scofield and Vincent J. Oliver, April 1977. (PB-270762)
- NESS 87 Atlantic Tropical and Subtropical Cyclone Classifications for 1976. D. C. Gaby, J. B. Lushine, B. M. Mayfield, S. C. Pearce, K. O. Poteat, and F. E. Torres, May, 1977. (PB-269674)
- NESS 88 NOAA CATALOG OF Products. Dennis C. Dismachek, Editor. June 1977. (PB-271315)
- NESS 89 A Laser Method of Observing Surface Pressure and Pressure-Altitude and Temperature Profiles of the Troposphere From Satellites. William L. Smith and C. M. R. Platt, July 1977, 38 pp. (PB-272660)
- NESS 90 Lake Erie Ice: Winter 1975-76. Jenifer H. Wartha, August 1977, 68 pp. (PB-276-386)
- NESS 91 In-Orbit Storage of NOAA/NESS Stand-by Satellites. Bruce Sharts, September 1977, 3 pp.
- NESS 92 Publications and Final Reports on Contracts and Grants, NESS - 1976. Catherine M. Frain, Compiler, August 1977, 11 pp. (PB-273169)
- NESS 93 Computations of Solar Insolation at Boulder, Colorado. Joseph H. Pope, September 1977, 13 pp. (PB-273-679)
- NESS 94 A Report on the Chesapeake Bay Region Nowcasting Experiment. Roderick A. Scofield and Carl E. Weiss, December 1977, 52 pp. (PB-277-102)
- NESS 95 The TIROS-N/NOAA A-G Satellite Series. Arthur Schwalb, March 1978, 75 pp.